Applied Environmental Research
- RESEARCH FOR SUSTAINABLE PLANET -

Research Article

Numerical Dose Assessment and Short-term Radioactivity Impact on Foodstuff for Continuous Release from of TRIGA Mark II Research Reactor

Ahmed Dahia*, Amel Dadda, Amina Lyria Cheridi Deghal, Abdellah Bouam

Nuclear Research Centre of Birine, B.P 180, Ain-Oussera 17200, Djelfa, Algeria

*Correspondence Email: dahia.univ@gmail.com

Abstract

This work is a contribution to the assessment of the radiological consequences of radioactivity and radiation dose for TRIGA Mark II research reactor during continuous operation. The potential release to the atmosphere of ^{131}I, ^{137}Cs, and ^{90}Sr are computed in the South direction is calculated using CROM software. We have attempted to evaluate the daily concentration of radioactivity and its impact on foodstuff. The annual average dose received from internal and external irradiation by age group through the different pathways were also considered. The simulation results showed that the highest air concentration was found at 225 m distance from the source and the calculated doses were found to be significantly very low. The contribution of Iodine ^{131}I is significantly higher in fruit vegetables, while the ^{137}Cs and ^{90}Sr are dominant in animal products. Furthermore, inhalation and ingestion of contaminated food were found to be the most likely routes of entry into the human body.

ARTICLE HISTORY
Received: 23 Nov. 2023
Accepted: 8 Mar. 2024
Published: 23 May 2024

KEYWORDS
CROM;
Radioactivity;
TRIGA;
Research reactor;
Dose

Introduction

The radioactive materials released into the atmosphere under normal operating conditions or under accidental conditions of a nuclear reactor are more influenced by the environmental conditions, which contributes to their dispersion and deposition on the ground resulting in the contamination of vegetation and the exposure of the public through various pathways. Noble gases, halogens, alkali metals, tellurium, Br-Sr nuclide, characterise the main important radioactive materials affecting the ambient atmosphere.

In recent decades, especially after the Chernobyl and Fukushima Daiichi nuclear accidents in 1986 and 2011 respectively, more original research has been carried out to calculate the radioactivity of the released material and to estimate the most serious radiological hazard risks for human health and to the environment. Alexakhin et al. [1] describe the distribution, migration, and environmental and agricultural impacts of the deposited radionuclides resulting from the Chernobyl accident and define the influence of their behaviour in human organisms and ecosystem. Morino, et al. [2] simulate the transport and deposition of radioactive materials and their interaction processes with oceans, land, and vegetation by using the ECHAM5 model. Christoudias and Lelieveld [3] estimated the cumulative inhalation doses from of the Fukushima Daiichi accident and the effective doses over 50 years based on the emission inventory reported by Stohl et al. [4]. Brandt et al. [5] used the Danish Rimpuff and Eulerian Accidental Release Model (DREAM) to predict the transfer of ^{131}I and ^{137}Cs from the Atmosphere through agricultural food chains using Chernobyl fallout. John et al. [6] defined methods for radiological risk assessment and environmental analysis for individuals exposed to radioactive elements near nuclear facilities. Hikaru et al. [7] conducted a study on the radiological aspects of fallout from the Fukushima Daiichi nuclear power plant accident by measuring radiation in the Chiba metropolitan area from March 15th, 2011. Malek, et al. [8] conducted another study to evaluate the radiological doses resulting from the deposition of

https://doi.org/10.35762/AER.2024018

^{131}I, ^{132}I, ^{133}I, ^{134}I, and ^{135}I on the ground, vegetation, milk, and meat in the event of a hypothetical accident involving a TRIGA research reactor. The study found that ^{131}I contributes the most to the dose in vegetation compared to all other radionuclides. Mizanur et al. [9] evaluated the radiological effects of Cs-137 and Sr-90 deposition on the ground, vegetation, milk, and meat. The study examined various pathways and air concentrations of accumulated radionuclides at the same reactor. The results showed that that the dose rates for members of the public were below the acceptable limits. Mollah et al. [10] studied the radioactivity and radiation levels in the vicinity of a proposed 600 MWe power plant at Rooppur site. The study found that the contamination levels in the soil and water were below the detection limit.

In this context, the Screening Model for Environmental Assessment CROM (Figure 1) [11] was used to predict the radiological consequences of the main doses due to external and internal irradiation doses for reference individuals mentioned cited in the International Commission on Radiological Protection (ICRP) publication 60 [12]. CROM's transport model includes modules for emission, diffusion, dry and wet deposition, and various exposure routes [13–14]. The used models are mainly based on IAEA Safety Report Series N° 19, with some additional improvements based on the methodology for assessing the radiological consequences of routine releases of radionuclides to the environment reported by RP-72 (EUR-15760) [15–17].

The study will assess the impact of the release of ^{131}I, ^{137}C and ^{90}Sr radioisotopes of nuclear material through the stack, which poses serious radiological hazards. We calculated the airborne fraction of these isotopes remaining to be released into the atmosphere from the 3MW(t) research reactor TRIGA Mark-II, which will be operate for 10 days. Our results were compared with some findings from the bibliography [8–9]. To elaborate on this work, we need to specify certain parameters in advance. These include the source term of the reactor core, the discharge rates for different releases, types of radionuclides to be discharged, geometry criteria, and meteorological conditions. Based on the calculations, we aim to define the most dominant route of exposure on individuals for hypothetical critical groups of the population living near the reactor site.

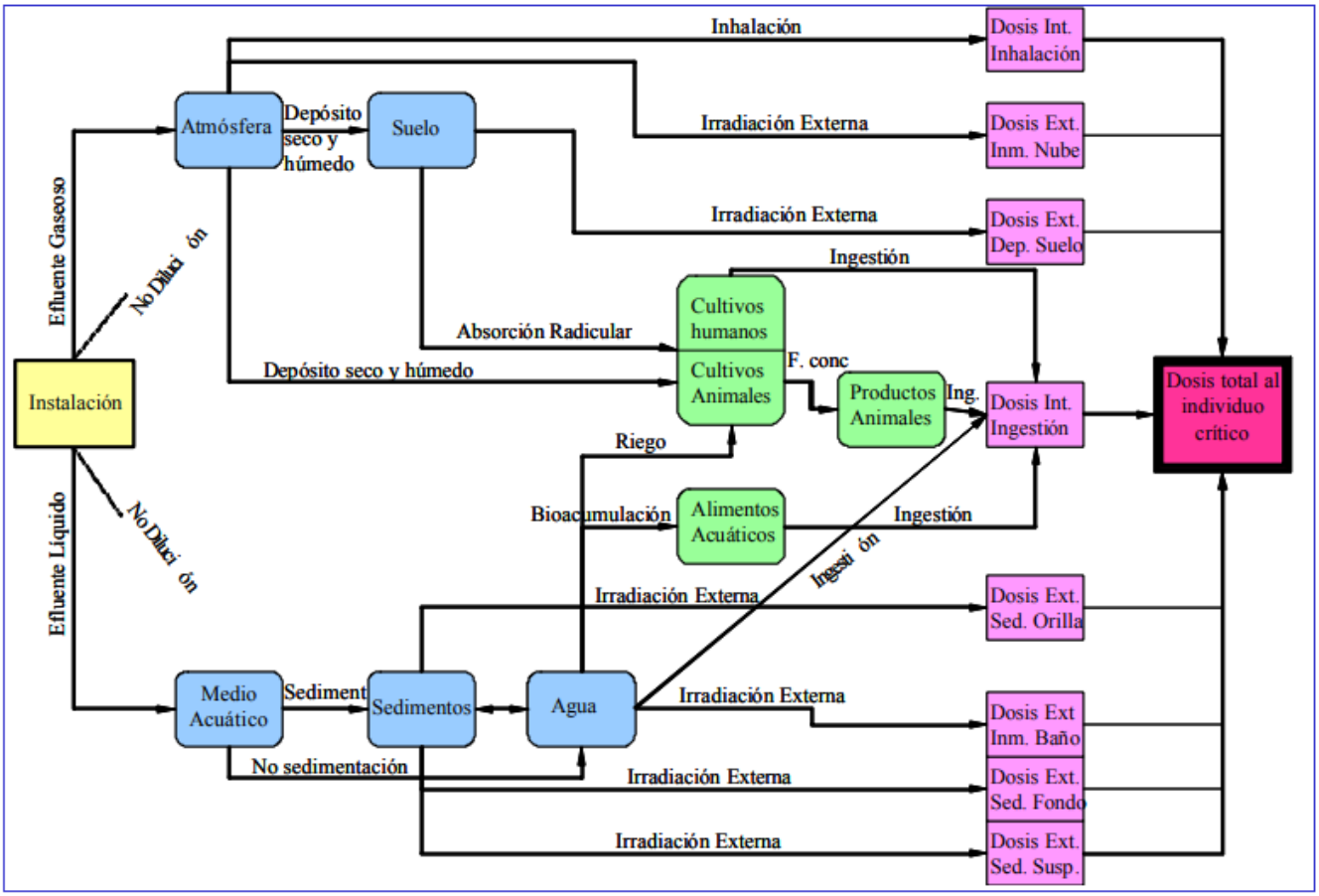

Figure 1 Overview of the conceptual model in CROM code [11, 18].

Material & methods

1) Site description and meteorological conditions

This study focused on the 3 MW TRIGA Mark II research reactor located in Savar, Dhaka. The facility uses a uranium-zirconium hybrid fuel moderated and light water-cooled system, which is used primarily for training and research in various fields, such as Neutron Activation Analysis (NAA), Neutron Radiography (NRG), Neutron Scattering (NS), and production of radioisotopes (^{131}I, ^{99}mTc, ^{46}Sc) for medical applications [19–22]. The meteorological observations at the site show that wind predominantly flows from the south (S) direction is dominant (Figure 2). Figure 3 displays the average wind speeds measured hourly at a height of 10 m for various directions. The mean activity concentration and dose calculations were evaluated based on a release height stack of approximately 32.36 m and the dominant stability class B (unstable) [8].

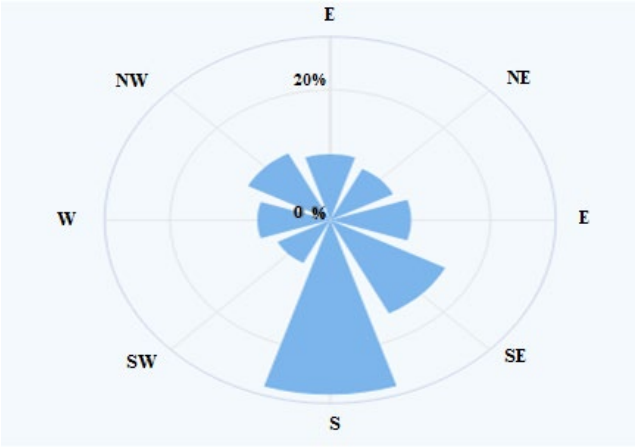

Figure 2 Wind rose at the nuclear Facility for 16 directional areas [23].

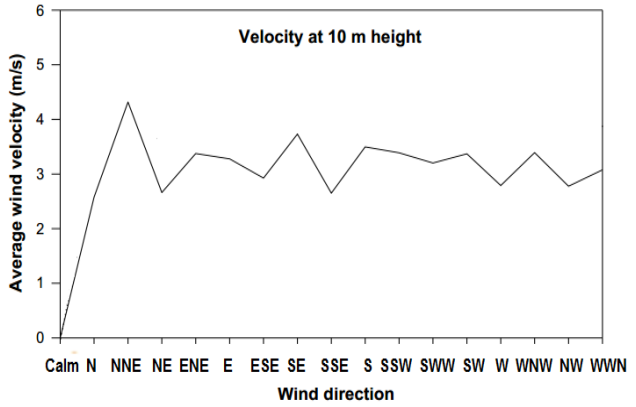

Figure 3 Average wind speed for various directions [8].

2) Released inventory

Table 1 illustrates the inventories of the most important radioelements in the reactor core and the corresponding activity released into the atmosphere. Following a continuous operation, a significant portion of the core inventory could be escaped and released into the atmosphere. The calculation only the fission products of Iodine radioisotope ^{131}I, ^{137}Cs, and ^{90}Sr. These nuclides were selected based on their physical and chemical properties, volatility, and their contribution to collective dose, particularly in the thyroid gland [24]. The calculation considers release fractions indicated in the US-NRC regulatory guide 1.183 and described in WASH-1400 (NUREG-75/014) document [25–26]. According to Shoaib and Iqbal [27], the release fractions on research reactors are 100% for noble gases, 40% for halogens, 30% for alkali metal, 5% for tellurium group, and 2% for Ba-Sr group. Table 1 specifies the core inventory and release rate of radioelements, assuming full power of 3 MW(t), approximately 30 days after start-up of irradiation, and 10 days of continuous operation at full power.

We consider the following assumptions for calculating the present work:

- Full power operation reactor: 3 MW (t),
- Time after the start of irradiation: 10 days,
- Continuous operation at full power: 10 days,
- Radionuclides considered: ^{131}I, ^{137}Cs, and ^{90}Sr,
- Fraction release: ^{131}I: 40%, ^{137}Cs: 30% and ^{90}Sr: 2 %,
- Leakage rate parameter, 1.157×10^{-7} 1/s. i.e., 1% /day,
- Calculation is made 2 hours after the start of release.

Table 1 Radionuclide inventory in the core, and activity released to the atmosphere [8–9]

Nuclide	Group	Total activity in core (kBq)	Released rate (Bq s^{-1})
^{131}I	Halogen	1.507E12	6.96E7
^{137}Cs	Alkali metal	3.393E9	3.92E3
^{90}Sr	Br-Sr group	3.543E9	4.09E3

3) Radiological concentration calculation

After being released into the atmosphere, nuclear material is transported by the wind in various directions and deposited onto the ground through wet and dry deposition. To determine the activity characteristics of the material to be discharged and dispersed in the air, the Gaussian approach described below in Eq. 1 is used to determine the average radionuclide concentration in the air [28]. Therefore, we determine all significant exposure pathways through which the discharged radionuclides can cause public exposure. We will estimate the annual average radionuclide concentrations in the air as follows [29–30]:

$$C_A = \frac{P_p Q_i}{U} \quad \text{(Eq. 1)}$$

Where; C_A is the ground level air concentration at downwind distance (Bq m^{-3}), Q_i is the average release rate for radionuclide i (Bq s^{-1}). A value of P_p was assigned for screening purpose [13].

4) Ground deposition calculation

The deposition of the radioactive material on the ground significantly effects human and animal feed. This is because the ingestion process which easily influences the transfer of radioactive material inside the human body. The deposition coefficient calculated by the Eq. 2, depends essentially on the nature of the selective radioactive material and the amount of the deposited activity per unit time at ground level [31].

$$\dot{d} = (V_d + V_{wt})C_A \quad \text{(Eq. 2)}$$

With $\dot{d}_i$ is the daily average deposit rate for a given radionuclide i in (Bq m^{-2} day^{-1}), V_d and V_{wt} are the dry and wet deposition coefficient, respectively (m day^{-1}). The total deposition coefficient $V_T = V_d + V_{wt}$ of 1000 m day^{-1} should be chosen for screening use for deposition of aerosols and reactive gases, which are corresponds to values for cesium and iodine fallout resulting from Chernobyl Nuclear Power Plant (NPP) accident [32–34].

5) Concentration calculation in vegetation and animal products:

5.1) Concentrations in vegetation

To estimate the concentration of radioactive materials deposited on vegetation due to direct contamination, the following equation was used [13]. The public is exposed to radiation by ingestion process from contaminated soil, which contains radionuclides that are redistributed within the plant and roots.

$$C_{v,i,l} = \frac{\dot{d}_i \alpha \left[1 - \exp\left(-\lambda_{E_i^v} t_e\right)\right]}{\lambda_{E_i^v}} \quad \text{(Eq. 3)}$$

With; $C_{v,i,l}$ is the fresh matter for vegetation consumed by humans (Bq kg^{-1}), α is the deposited activity fraction (m^2 kg^{-1}), $\lambda_{E_i^v}$ is the effective rate constant for reduction of activity of any radionuclide (day^{-1}), t_e is the time period that the cultivated plant are exposed to contamination during the growing season (day).

5.2) Concentrations in animal feed

Additionally, the concentration can be affected by the ingestion of contaminated foodstuffs and other environmental materials by animals. The concentration of radionuclides in animal feeds is influenced by various factors, including the animal species, its mass, age, growth rate, and the digestibility of the feed. The taken time between harvest and consumption of food is 14 days, and the amount of the feed consumed by the animal is 16 kg day^{-1}. The concentration in animal feed can be calculated using the following Eq. 4:

$$C_{a,i} = f_p C_{v,i} + (1 - f_p) C_{p,i} \quad \text{(Eq. 4)}$$

Where; $C_{a,i}$ is the concentration of radionuclide in the animal feed (Bq kg^{-1}), $C_{v,i}$ is the concentration of radionuclide for pasture (Bq kg^{-1}), $C_{p,i}$ is the concentration of radionuclide in stored feed t_h = 90 days (Bq kg^{-1}), f_p is the fraction that animals consume fresh pasture vegetation, in our case is 0.7 [11, 32].

5.3) Concentration in meat and milk

The radioactivity concentration in meat and milk reflects the proportion of the year during which animals consume fresh or stored pasture, as well as their intakes of water and dry matter. Eq. 5 describes the concentration of radionuclide in meat.

$$C_{f,i} = F_m \left(C_{a,i} Q_f + C_{w,i} Q_w\right) \exp\left(-\lambda_i t_f\right) \quad \text{(Eq. 5)}$$

Where; $C_{f,i}$ is the concentration of radionuclide in animal flesh (Bq kg^{-1}), $C_{a,i}$ is the concentration of radionuclide in animal feed (Bq kg^{-1}), $C_{w,i}$ is the concentration of radionuclide in water in (Bq m^{-1}), F_m is the fraction of the animal's daily intake of a nuclide (day kg^{-1}), Q_f is the feed amount consumed by the animal in (kg day^{-1}), Q_w is the amount of water consumed by the animal (m^{-3} day^{-1}), and t_f is the average time between slaughter and human consumption of meat (day).

6) Dose calculation

6.1) Calculation of internal dose intake by inhalation and ingestion

The doses are evaluated for six age groups, as recommended by the International Commission for Radiological Protection (ICRP) [12], due to internal exposure from ingesting food or inhaling. The critical groups, which are expected to receive the highest dose from the source, are reasonably homogeneous with respect to all those factors that significantly influence the received dose. The child dose coefficients are generally higher than those for adults [13]. The annual effective dose from inhaling and ingesting food for each radionuclide and each age group is calculated using the following expressions (Sv a^{-1}):

$$E_{inh} = C_A R_{inh} DF_{inh} \quad \text{(Eq. 6)}$$

$$E_{ing,i} = C_{p,g,i} DF_{ing} H_p \quad \text{(Eq. 7)}$$

Where; C_A is the concentration in air (Bq m^{-3}), R_{inh} is the inhalation rate (m^3 a^{-1}), DF_{inh} and DF_{ing} are the inhalation and ingestion dose coefficient (Sv Bq^{-1}), respectively. $C_{p,g,i}$ is the concentration of radionuclide

in foodstuff at the time of consumption (Bq m^{-1}), H_p is the consumption rate for foodstuff (kg a^{-1}).

6.2) External dose calculation from ground deposition

The annual effective dose from ground deposition Eg,r (Sv a^{-1}) for each radionuclide and each age group is given by:

$$E_{g,r} = C_{g,r} DF_{inh} O_f \quad \text{(Eq. 8)}$$

Where; DF_{gr} is the dose coefficient for exposure to ground deposits (Sv/year per Bq m^{-2}), O_f is the fraction of which the hypothetical critical group member is exposed to this particular pathway, $C_{g,r}$ is the deposition density of radionuclide (Bq m^{-2}) obtained from the ground deposition expression (Eq. 2).

Results and discussions

A numerical study was conducted to determine the concentration of air and deposition, and the resulting radiation doses due to external and internal exposure from continuous release using CROM code. The radionuclides Iodine ^{131}I, the Alkali metal ^{137}Cs, and ^{90}Sr radionuclides were computed using a Gaussian distribution for all wind directions. The maximum annual activity concentration and deposition to the ground of each radionuclide, listed in Table 1, depends on the release fraction of the reactor core inventory.

The air concentrations and the total deposition were calculated as a function of downwind distance for the moderately unstable class "B" in the dominant South direction. The total doses of internal and external exposure pathways were estimated for different foodstuff (human vegetables, animal feed) and animal products (milk and meat). The horizontal distribution pattern of the mean concentration and the total dose by age group are presented in histogram forms. The population is divided into six representative critical groups: 0-1 year, 1-2 years, 2-7 years, 7-12 years, 12-17 years, and adults (over 17 years).

1) Air concentration and deposition calculations

Figure 4 provides an overview of the temporal variation of air concentration and ground deposition of radioactive pollutants in the south (S) wind direction. ^{131}I is the most common fission product, produced in large quantities in nuclear reactors. It is a radioisotope with a very short half-life of eight days, decaying by β^- radiation into ^{131}Xe, the most powerful neutron absorber in a reactor, and also a γ-rays emitter. Upon calculation, it's evident that the activity concentration of ^{131}I is higher than that of other radioelements. Its maximum activity concentration was estimated at 2.177 kBq m^{-3}, while its deposition is about 2.177E3 kBq m^{-2} per day. The concentrations of ^{137}Cs and ^{90}Sr were found to be less significant due to their low emission rates (Figure 4a). Therefore, we can observe that the activity concentration is influenced by the half-life of each radioelement. Short-lived isotopes, such as Iodine, have a greater impact on the radioactivity effect. Additionally, the duration of contamination for most of these elements is brief. Contrarily, ^{137}Cs and ^{90}Sr represent the majority of residual contamination in the environment due to their half-lives of 30 years and 28 years respectively. These elements tend to remain on the ground, leading to prolonged contamination and concentration in the food chain. Figure 4(b) displays the plume centrelines ground deposition, which follows a similar trend as the mean activity concentration in air curves shown in Figure 4(a).

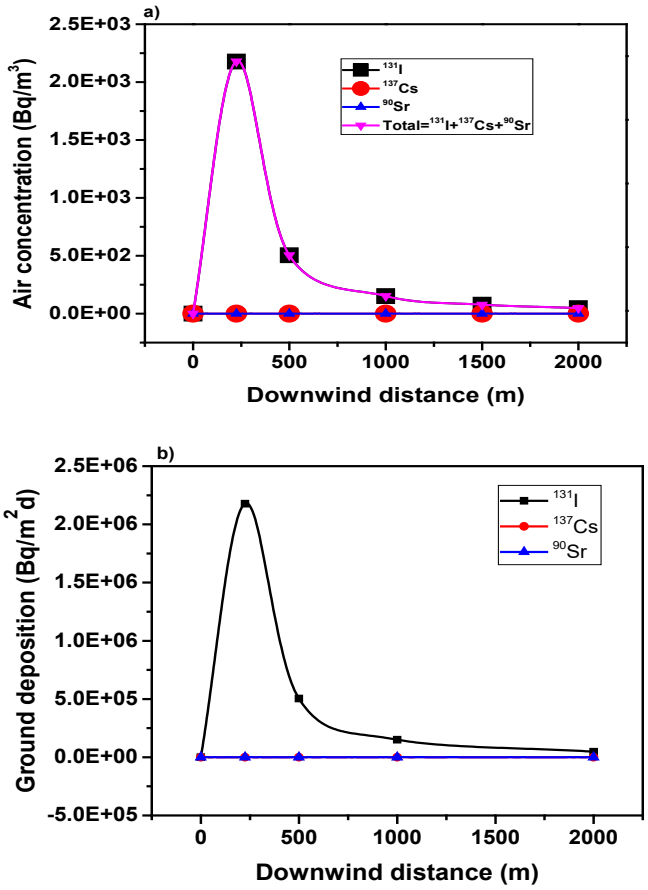

Figure 4 Plots of a) mean activity concentration in air, and b) ground deposition as a function of downwind distance.

Following this, a histogram classification form was used to classify and compare the mean activity concentration levels of ^{131}I, ^{137}Cs, and ^{90}Sr radionuclides in the air at different downwind distances (see Figure 5). We can observe, that the concentration level is highest at a downwind distance of 225m, after which the

radioactivity of the plume decreases significantly due to radioactive decay.

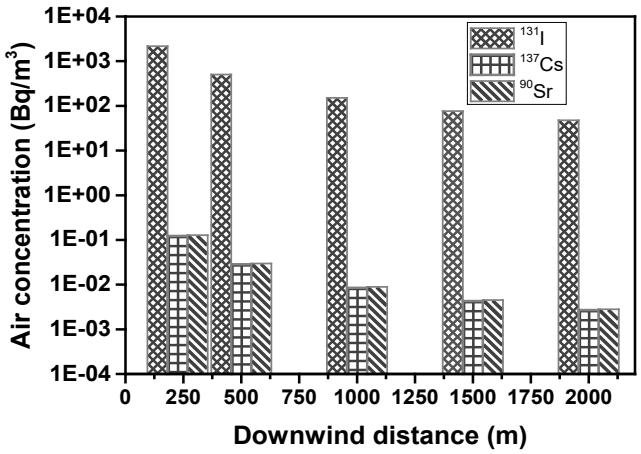

Figure 5 A comparison of different levels of the mean activity concentration in air as a function of downwind distance.

Figure 6 illustrates air concentrations calculated for 16 directions up to 2000 m from the reactor site. The dominant radioisotope in all directions is ^{131}I due to its high emission rate of 6.965E4 kBq m^{-3} and diffusivity in the air. Its radioactivity reaches a value of 3.175 kBq m^{-3} in the north (N) direction.

2) External exposure due to feed consumption

Figure 7 depicts the calculated concentrations of airborne radionuclides deposited on the ground in the south direction at 225m downwind distance. The figure illustrates the activity levels in human vegetables (fruit vegetables), animal vegetables (pasture), and animal products (meat and milk) due to the ingestion of radioactive materials transferred from plants and then to meat and milk. The ^{137}Cs nuclide is absorbed into the soil quickly and is less available for plant uptake, while the 90Sr is more mobile and migrates downward into the soil.

The results show that ^{131}I is the main contaminant in vegetation and animal products, while ^{137}Cs and ^{90}Sr are significant in animal products. Milk, which is the main source of thyroid contamination, has the highest concentration of ^{131}I about 6.750E3 kBq kg^{-1}. Meat and Milk have similar level of concentration of ^{137}Cs and ^{90}Sr. ^{131}I is also present in fruits vegetables and pasture, with a maximum radioactivity concentration of 1.436E2 and 1.407E3 kBq kg^{-1}, respectively. The variations in the results are due to different processes that contribute to the transfer of radioactivity.

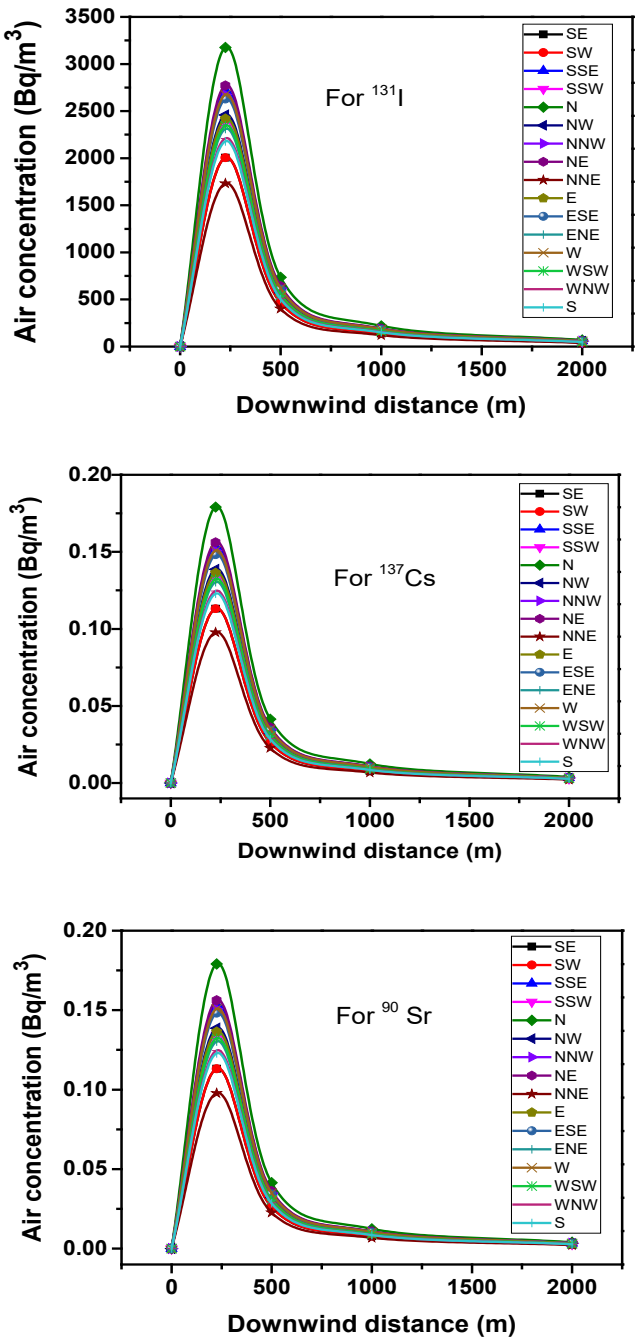

Figure 6 Air concentration of ^{131}I, ^{137}Cs and ^{90}Sr radionuclides at 16 directions as a function of downwind distance.

3) Dose calculation

To assess the doses resulting from internal and external exposure to radioactive material discharges in the environment, we have evaluated the public's exposure, taking into account the age of the representative exposed person. Inhalation and the ingestion of contaminated food are considered the most probable routes ofentry into the human body.

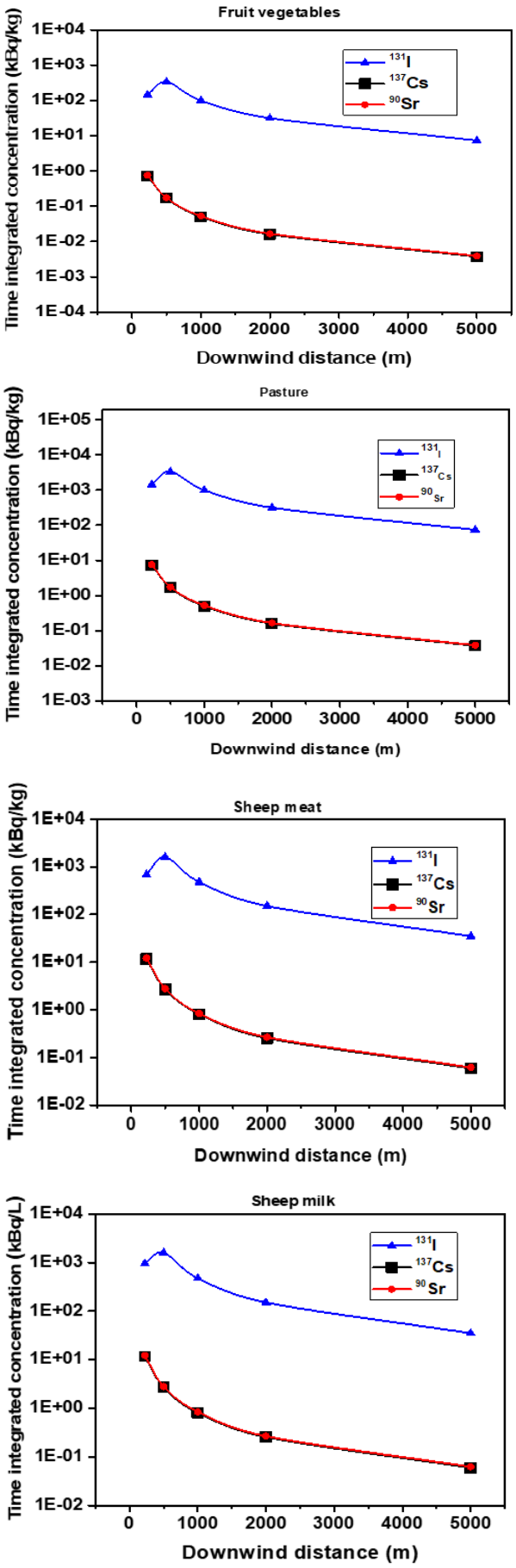

Figure 7 Predicted concentration and distance dependence for the transfer of ^{131}I, ^{137}Cs, and ^{90}Sr to human food stuff, animal vegetables and animal products.

The radiation dose from inhalation and ingestion is mainly attributable to the activity deposited on the ground and absorbed by plants. This significantly contributes to internal radiation exposure [10].

The initial simulation results show that for children aged 1-2 years who received the highest doses in the close vicinity of the source at 0.225 km in the south direction, the maximum doses received by inhalation and ingestion were equal to 0.297 and 124.2 mSv a^{-1}, respectively, for ^{131}I. In the same conditions and for the same age group, the smallest values received were about 4.7E-6 and 0.038 mSv a^{-1} of ^{137}Cs (Figure 8). The presence of milk in food rations is responsible for these finding. It is important to note that ^{131}I and ^{137}Cs are the primary sources of internal radiation doses in the Fukushima Daiichi accident, with 70% caused by ^{131}I and 30% caused by ^{137}Cs [4]. All of these values are below the annual dose regulatory limit of 1 mSv for the public asset, as stated in IAEA Safety Report Series number 115 [35], and the ICRP recommendations [12, 32, 36]. This situation does not pose a health risk to individuals who will not be affected by radiation exposure during the plume passage. Therefore, emergency interventions or countermeasures, such as evacuation and the supply of iodine tablets, should not be required.

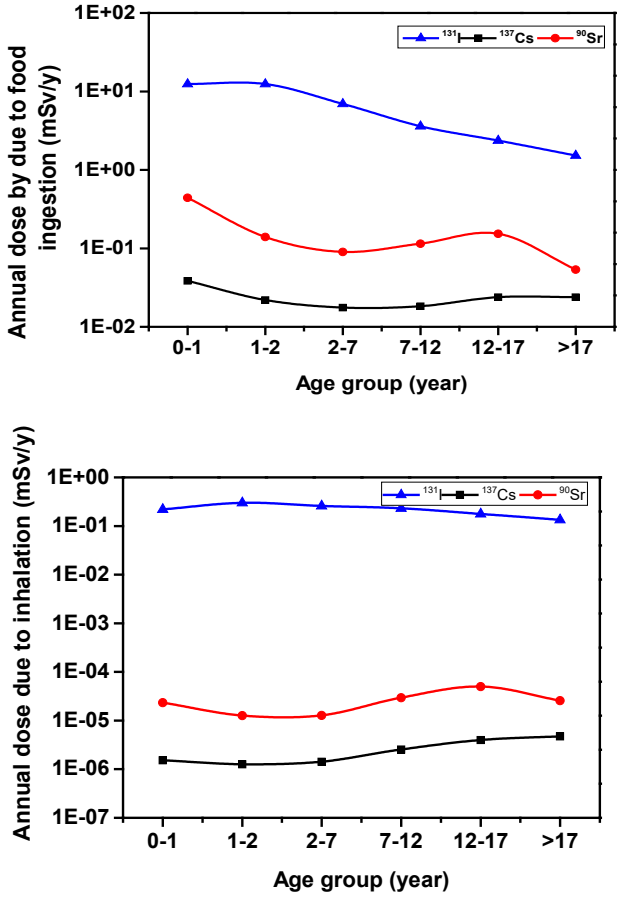

Figure 8 Dose calculation received by internal irradiation by age groups.

Additionally, to provide the most accurate description of the doses, the Health Physics Code Hot Spot [37] of Lawrence Livermore National Laboratory (LLNL laboratory was used to display the boundary contour line areas of the doses at the release location in Google Earth, using geographical coordinates of the 3 MW Triga Mark II reactor. There are three marked contours with different colours; the red contour represents the highest dose risk for the population in the inner area, while the green and blue contours represent the middle and outer doses [38]. The area is divided into three distinct regions, each marked with a different colour contour. 0.06 km^2, 0.66 km^2, and 9.4 km^2 for ^{131}I; 0.34 km^2, 3.7 km^2, and 39 km^2 for ^{137}Cs; 0.10 km^2, 1.2 km^2, and 13 km^2 for ^{90}Sr (Figure 9). Figure 10 shows the maximum distances from the source to the axial limit of the contour lines in the downwind direction; for Iodine 131 (Red: 0.640km, green: 2.2km, bleu: 7.6km), for Cesium 137 (Red: 1.4km, green: 4.6km, bleu: 17km), and for Strontium 90 (Red: 0.77km, green: 2.6km, bleu: 9.1km).

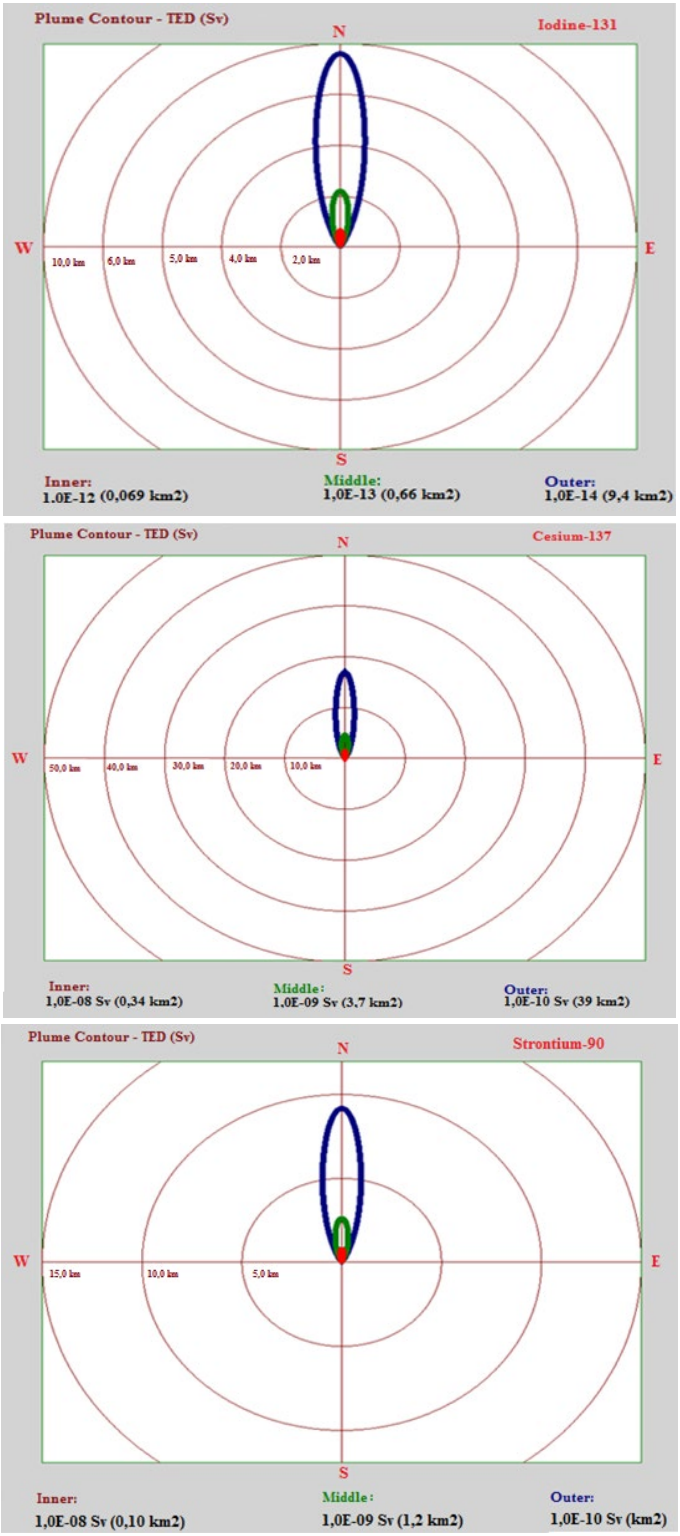

Figure 9 Plume contour lines of ^{131}I, ^{137}Cs, and ^{90}Sr as a function of downwind distance.

Figure 10 Maps of the boundary contour line areas of the doses at the reactor release location in Google Earth.

Figure 11 provides an overview of the total annual dose, including internal and external radiation exposure. As indicate in the results mentioned above that the inhalation and ingestion are the primary routes of contamination for human organs.

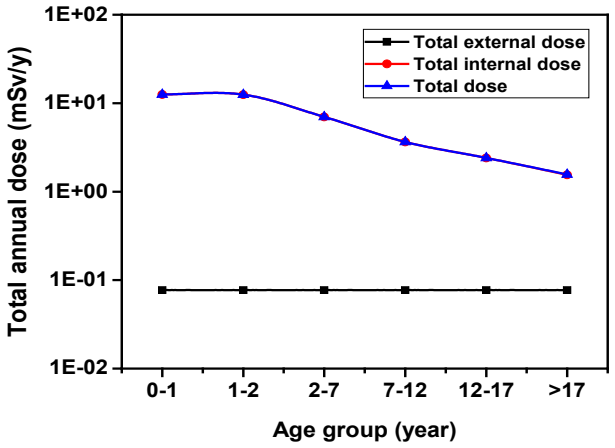

Figure 11 Total annual dose by age groups.

Figure 12 displays histograms of the probabilistic distributions of total dose by age group for various radionuclides relevant to this study. These distributions delineate the average values that can be attributed to dose. Approximately 18.7% of the mean dose contribution falls within an interval ranging from 5.581 mSv to 3.013 mSv for the critical age group of 0 to 1 year. For the age group of 1–2 years, the dose contribution, approximately 16.5% for a range of 2.833 to 5.85 mSv. Similary, for the age group above 17 years, the contribution varies within the same range with a lower dose interval.

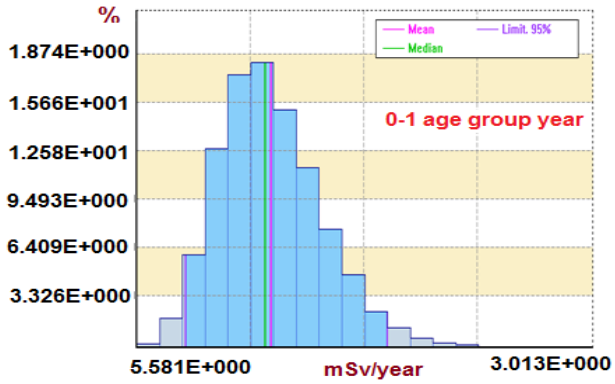

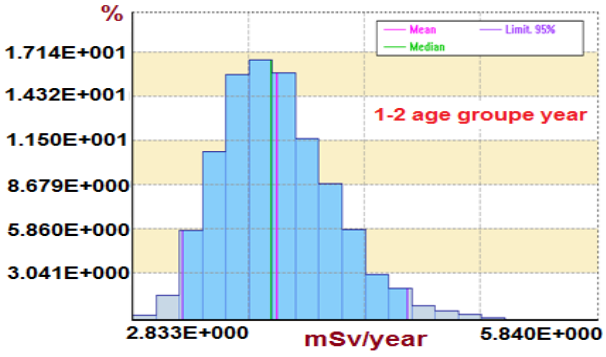

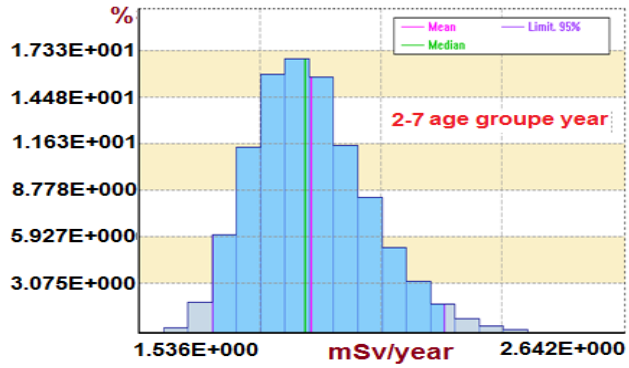

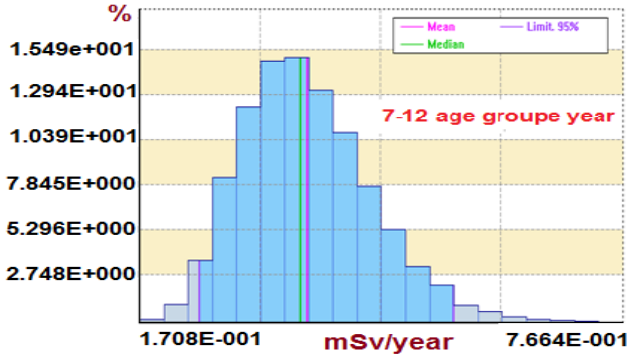

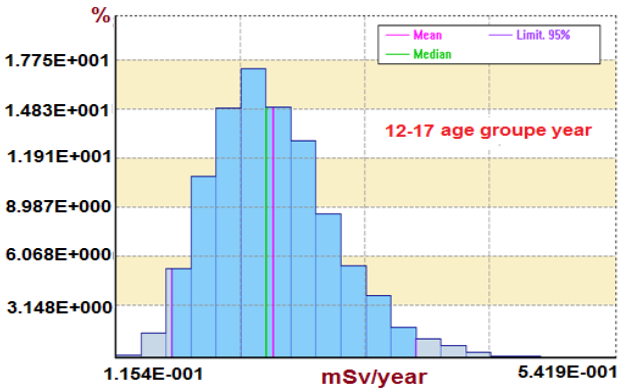

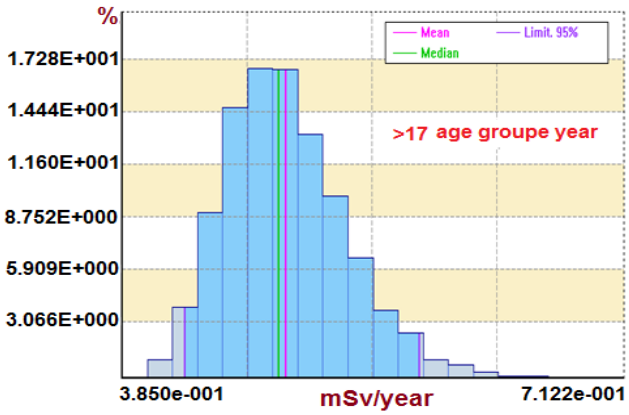

Figure 12 Time variations at Log-normal probability distribution of ^{131}I, ^{137}Cs and ^{90}Sr radionuclides assigned to total dose parameter by age groups.

Figure 13 provides an overview of the relative contribution of radionuclides to total dose via various pathways in the South direction. Ground deposition, inhalation, and immersion are the main pathways contributing to total dose contribution. The data shows that ^{131}I is the dominant contributor in animal products, particularly in milk accounting for 75.05%, followed

by ^{137}Cs (61.53%) and ^{90}Sr (49.94%). Meat samples have been found to contain ^{131}I at 6.271%, ^{137}Cs at 37.938%, and ^{90}Sr at 49.629%. The study also identified the contributions of all radionuclides in immersion and inhalation.

Based on the results, it can be concluded that ^{131}I is the most dominant contributor to radioactivity and doses compared to the other radionuclides. When animal ingest iodine deposited on the grass during lactation, it quickly appears in their milk. This occurs within a few hours of ingestion, with the maximum amount appearing after three days.

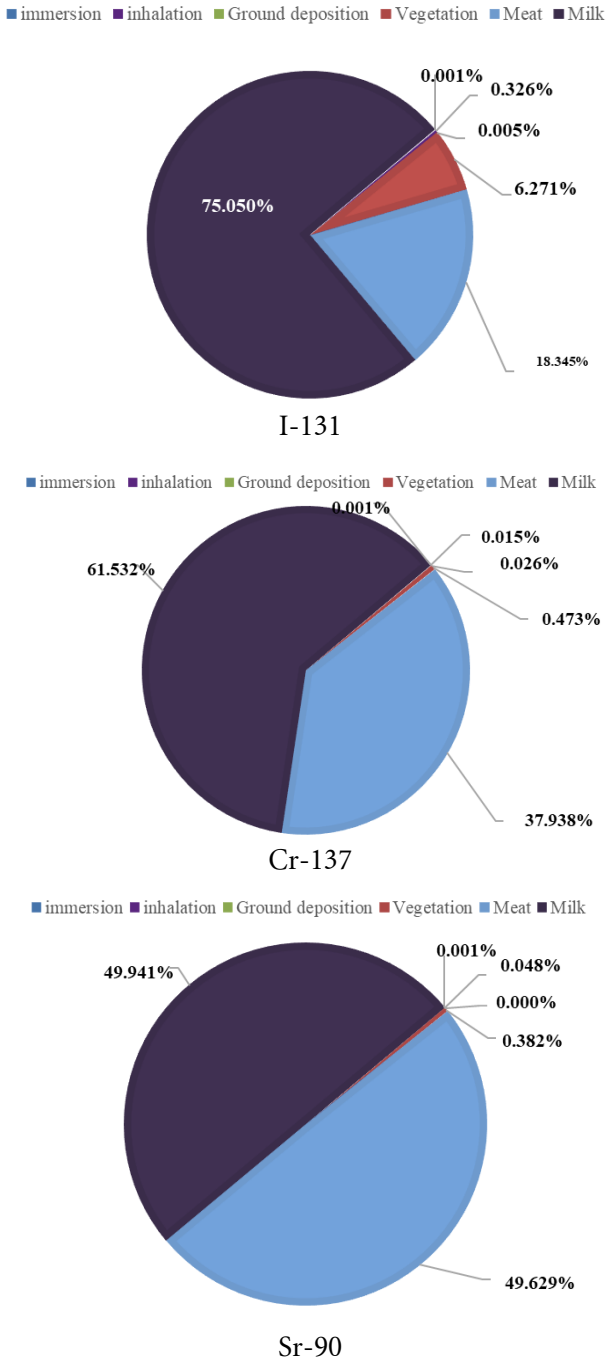

Figure 13 Dose contribution (%) of all radionuclides contributing to dose pathways in south direction.

Conclusion

This work attempts to simulate the release of ^{131}I, ^{137}Cs, and ^{90}Sr radionuclides from a 3MW research reactor in the South wind direction using the Gaussian plume model CROM for environmental assessment. The atmospheric radionuclide concentration and deposition through different pathways were calculated. It is noteworthy that short-lived isotopes, such as ^{131}I, have a greater impact on radioactivity and exhibit higher activity compared to other radioisotopes.

The study determined the activity concentration of radionuclides in human vegetables (fruit vegetables), animal vegetables (pasture), and animal products (meat and milk). The results showed that ^{131}I had a significantly higher activity concentration than the other radionuclides in fruit vegetables and pasture, while ^{137}Cs and ^{90}Sr were more present in animal products (meat and milk).

Internal and external radiation doses to the public were also computed, taking into account the age of representative groups. It should be noted that the total doses due to inhalation and food ingestion were found to be 0.297 and 124.2 mSv a^{-1}, respectively, for ^{131}I applied to children between the ages of 1–2 years. These values are satisfactory as they are well below the annual dose regulatory limit of 1 mSv for personnel, as stated IAEA Safety Report Series number 115 and the ICRP recommendations. No emergency interventions or countermeasures are required as this situation does not pose a health risk to individuals.

Declaration of Interests

The authors declare that they have no known competing financial interests or personal relationships that could have appeared to influence the work reported in this paper.

Reference

[1] Alexakhin, R.M., Sanzharova, N.I., Fesenko, S.V., Spiridonov, S.I., Panov, A.V., Chernobyl radionuclide describes distribution, migration, and environmental and agricultural impacts. Health Physics, 2007, 93(5), 418–426.

[2] Morino, Y., Ohara, T., Nishizawa, M. Atmospheric behavior, deposition, and budget of radioactive materials from the Fukushima Daiichi nuclear power plant in March 2011. Geophysical Research Letters, 2011, 38(7), 1–7.

[3] Christoudias, T., Lelieveld, J. Modelling the global atmospheric transport and deposition of radionuclides from the Fukushima Daiichi nuclear accident. Atmospheric Chemistry and Physics, 2013, 13(3), 1425–1438.

[4] Stohl, A., Seibert, P., Wotawa, G., Arnold, D., Burkhart, J.F., Eckhardt, S., Yasunari, T.J. Xenon-133 and Caesium-137 releases into the atmosphere from the Fukushima Daiichi Nuclear Power Plant: Determination of the source term, atmospheric dispersion, and deposition. Atmospheric Chemistry and Physics, 2012, 12(5), 2313–2343.

[5] Brandt, J., Christensen, J.H., Frohn, L.M. Modelling transport and deposition of Caesium and Iodine from the Chernobyl accident using the DREAM model. Atmospheric Chemistry and Physics, 2002, 2(5), 397–417.

[6] John, E.T., Grogan, H.A. Radiological risk assessment and environmental analysis. Oxford University Press, Oxford, 2008, 360–380.

[7] Hikaru, A., Masakazu, A., Bi, C., Takao, K., Takeshi, K., Tomotaka, K., …, Yushu, W., Takao, M. Radiation measurementsin the Chiba metropolitan area and radiological aspects of fallout from the Fukushima Daiichi Nuclear Power Plants accident. Journal of Environmental Radioactivity, 2012, 111, 42–52.

[8] Malek, M.A., Chisty, K.J.A., Rahman, M.M. Dose distribution of ^{131}I, ^{132}I, ^{133}I, ^{134}I, and ^{135}I due to a hypothetical accident of TRIGA Mark-II research reactor. Journal of Modern Physics, 2012, 3, 1572–1585.

[9] Mizanur, R.A.F.M., Shakilur, R.Md., Selina, Y., Kutub, U. Assessment of radiological dose around a 3-MW TRIGA Mark-II Research Reactor. International Letters of Chemistry Physics and Astronomy, 2013, 10(2), 65–82.

[10] Mollah, A.S., Chakraborty, S.R. Radioactivity and radiation levels in and around the proposed Nuclear Power Plant site at Rooppur. Japanese Journal of Applied Physics, 2009, 44(4), 408–413.

[11] Juan, C.M., Beatriz, R., Tesus, R. CROM Code user's manual V8.2.5, Codigo de cRibapara evaluaciOn de iMpacto, Screening Model for Environmental Assessment. CIEMAT, Madrid, 2014. [Online] Available from: https://www-pub.iaea.org/search/search.aspx?orig_q=RN:39043808.

[12] ICRP, International Commission on Radiological Protection. 1990 Recommendations of the International Commission on Radiological Protection, ICRP 60, Annals of ICRP, 1991, 21, 1–3.

[13] Kryshev, I.I., Makhonko, K.P., Sazykina, T.G. Dose assessment and reconstruction in the areas of Russia contaminated after the Chernobyl accident, 1994. IAEA-TECDOC-755, 105–114.

[14] Dahia, A., Merrouche, D., Djillali R.M., Rezoug, T, Aguedal, H. Numerical study of long-term radioactivity impact on foodstuff for accidental release using atmospheric dispersion model. Arabian Journal for Science and Engineering, 2018, 44, 5233–5244.

[15] IAEA, International Atomic Energy Agency. Generic models for use in assessing the impact of discharges of radioactive substances to the environment. Safety Reports Series No. 19, Vienna, 2001.

[16] Simmonds J.R., Lawson, G., Mayall, A. Methodology for assessing the radiological consequences of routine releases of radionuclides to the environment. Radiation Protection 72, Luxembourg, 1995, 351p.

[17] Simmonds, Webb, G., White, I., Bouville, A. The methodology for assessing the radiological consequences of routine releases of radionuclides to the environment used in PC-CREAM 08, 2009.

[18] Juan C.M. CROM: An introduction, Radiation protection for the public and the environment CIEMAT. Presentation, Vienna January 27th, 2011.

[19] Islam, M.S., Haque, M.M., Salam, M.A., Rahman, M.M., Khandokar, M.R.I., Sardar, M.A., …, Zulquarnain, M.A. Operation experience with the 3MW Triga Mark-II research reactor of Bangladesh. IAEN-CN-156.

[20] Haque, M.M., Zulquarnain, M.A., Salam, M.A. Strengthening operational safety of the 3MW TRIGA MK-II research reactor of Bangladesh Atomic Energy Commission through modification and upgrade of its water system. International Conference on topical issues in Nuclear Safety, Vienna, 2001.

[21] Zulquarnain, M.A., Haque, M.M., Salem, M.A., Islam, M.S., Saha, P.K., Sarder, M.A., …, Islam, N. Experience with the operation, maintenance and utilization of the 3 MW Triga Mark-II research reactor of Bangladesh. International Journal of Nuclear Energy Science and Technology, 2009, 4(4), 299–312.

[22] Hoq, M.A., Malek Soner, M.A., Rahman, A., Salam, M.A., Islam, S.M.A., Estimation of 41Ar activity concentration and release rate from the TRIGA Mark-II research reactor. Journal of Environmental Radioactivity, 2016, 153, 68–72.

[23] World Weather. Weather archive in Dhaka. [Online] Available from: https://world-weather.info/archive/bangladesh/dhaka/.

[24] Birikorang, S.A., Abrefah, R.G. Radiological dose assessment for Ghana Research Reactor-1 at shutdown using dispersion model: Conversion from high-enriched Uranium to Low-Enriched Uranium Fuel. Environmental Engineering and Management Journal, 2018, 74(1), 21–358.

[25] ICRP, US-NRC, Nuclear Regulatory Commission. Alternative radiological source terms for evaluating design basis accidents at Nuclear Power Reactors. Regulatory Guide 1.183, 2000.

[26] IAEA, International Atomic Energy Agency. Reactor safety study, An assessment of accident risks in U.S commercial nuclear power plant. Wash-1400 (NUREG 75/014), 1975.

[27] Shoaib, R.S., Iqbal, M. Atmospheric dispersion modeling for an accidental release from the Pakistan research reactor-1 (PARR-1). Annals of Nuclear Energy, 2005, 32(11), 1157–1166.

[28] Meng, D., Yang, L., Shen, F., Yang, Y., Ma, Y., Ma, T., …, Fu, C. Environment assessing for airborne radioactive particulate release-Introduction of methods in IAEA. Safety Report Series No. 19. Journal of Radiation Protection and Research, 2016, 41(4), 409–417.

[29] IAEA, International Atomic Energy Agency. Programmes and systems for source and environmental radiation monitoring. Safety Reports Series N° 64, Vienna-Austria, 2010, pp. 2–7.

[30] NCRP, National Council on Radiation Protection and Measurements. Screening techniques for determining compliance with environmental standards, releases of radionuclides to the atmosphere. NCRP Commentary No. 3, Revision Plus Addendum, Bethesda, 1996.

[31] Yasunari, T.J., Stohl, A., Ryugo S.H., John, F.B., Sabine, E., Tetsuzo, Y. Cesium-137 deposition and contamination of Japanese soils due to the Fukushima nuclear accident. Proceeding of the National Academy of Sciences, 2011, 108(49), 19530–19534.

[32] IAEA, International Atomic Energy Agency, Fundamental calculation model for the determination of the radiological effects inside and outside the research reactor after hypothetical accidents with release of high amount of fission products from the core. In: Research Reactor Core Conversion Guidebook, IAEA-TECDOC-643, Vienna 2, 1992, 211–232.

[33] IAEA, International Atomic Energy Agency. Generic models for use in assessing the impact of discharges of radioactive substances to the environment, Safety Reports Series No. 19, Vienna, 2001.

[34] Koehler, H., Peterson, S.R., Hoffman, F.O. (Eds). Multiple model testing using Chernobyl fallout data of ^{131}I in forage and milk and ^{137}Cs in forage, milk, beef and grain. BIOMOVS Tech. Rep. No. 13, Scenario A4, National Institute for Radiation Protection, Stockholm, 1991, 179.

[35] IAEA, International Atomic Energy Agency. International basic safety standards for protection against ionizing radiation and for the safety of radiation sources. Safety Report Series N° 115, Vienna, 1996.

[36] ICRP, International Commission on Radiological Protection. Human respiratory tract model for radiological protection. ICRP 66, Annals of ICRP, 1994, 24, 1–3.

[37] Homann, S.G., Aluzzi, F. HotSpot Health physics codes version 3.1.2 user's guide. LLNL-SM- 636474, National Atmospheric Release Advisory Center, Lawrence Livermore National Laboratory, Livermore, CA, USA, 2020.

[38] Dahia, A., Merrouche, D., Dadda A., Cheridi, A.L. Comparative radiation dose study of a hypothetical accident in a research reactor. Kemija u Industriji, 2022, 71(7–8), 429–438.